such as the current diagrammatic techniques.[5,7,10] In fact, it would be interesting to see if the latter give results (for cross sections, etc.) equivalent to those of the present canonical theory, in particular, if the radiative corrections are identical.[13]

Further research is clearly needed on all these points.

ACKNOWLEDGMENT

I am indebted to Professor C. W. Misner for many clarifying discussions, and to Professor J. Weber for the warm hospitality of the University of Maryland.

APPENDIX

Equation (12) can easily be proved from the identity

$$\delta y^A(\mathbf{x}')\equiv\int\frac{\delta y^A(\mathbf{x}')}{\delta g_{mn}(\mathbf{x})}\delta g_{mn}(\mathbf{x})d\mathbf{x}, \tag{99}$$

by considering infinitesimal distortions[18] $x^s\rightarrow x^s+z^s(\mathbf{x})$. We have

$$\delta g_{mn}=-g_{ms}z^s{}_{,n}-g_{ns}z^s{}_{,m}-g_{mn,s}z^s, \tag{100}$$

and, since y^A is a scalar field,

$$\delta y^A=-y^A{}_{,s}z^s. \tag{101}$$

Integration by parts of (99) then gives

$$-y^A{}_{,s}(\mathbf{x}')z^s(\mathbf{x}')=\int\left\{2\left[\frac{\delta y^A(\mathbf{x}')}{\delta g_{mn}(\mathbf{x})}\right]_{,n}g_{ms}(\mathbf{x})-\frac{\delta y^A(\mathbf{x}')}{\delta g_{mn}(\mathbf{x})}g_{mn,s}(\mathbf{x})\right\}z^s(\mathbf{x})d\mathbf{x}, \tag{102}$$

valid for arbitrary z^s, and Eq. (12) follows immediately.

PHYSICAL REVIEW VOLUME 171, NUMBER 5 25 JULY 1968

Antiprotons and Positrons in Cosmic Rays*

C. S. SHEN

Department of Physics and Department of Geoscience, Purdue University, Lafayette, Indiana 47907

AND

G. B. BERKEY

Department of Physics, Purdue University, Lafayette, Indiana 47907

(Received 29 February 1968)

The antiproton flux in primary cosmic rays is treated by calculating the ratio of antiproton to positron production in nuclear collisions. It is shown that in the few-BeV energy range at earth, the ratio of the antiproton flux to the positron flux is given directly by their production-cross-section ratio and is independent of astronomical uncertainties. At higher energy, the equilibrium intensity ratio deviates from the production ratio due to modulation in interstellar space. The antiproton production cross section is deduced from the pion production cross section on the basis of a simple physical argument. By comparison with the observed positron intensity, we obtain an antiproton flux which is approximately 10^{-4} of the proton flux for $E\geq 5$ BeV and falls off rapidly below 2 BeV. It is suggested that a detection of cosmic-ray antiprotons in the lower energy range would test the validity of the nuclear-interaction model used in the calculation, while extension of the measurements to higher energies, which is perhaps difficult experimentally at present, would serve as a useful probe in the study of the origin and propagation of secondary cosmic-ray particles.

IN this paper we calculate the ratio of the antiproton to positron flux in primary cosmic rays. They are secondary particles[1] produced by collisions of cosmic-ray nuclei with the 3 g/cm^2 of matter they have traversed. While attempts to detect antiprotons have yielded only upper limits,[2] the presence of cosmic-ray positrons is now well established.[3] In studying the production of secondary particles in space, one encounters difficulties in two areas. The first is in astrophysics, where the density and composition of the ambient gases is poorly known, and the details of cosmic-ray propagation and confinement are uncertain. The other is in nuclear physics, where knowledge of the production cross section for antiprotons is lacking. Such uncertainties have limited the accuracy of theoretical calculations

* Work supported by National Aeronautical and Space Administration Grant No. 5270-52-3969.

[1] Cosmic-ray antiprotons may also be produced by direct acceleration in regions consisting of antimatter [see H. Alfvén, Rev. Mod. Phys. **37**, 652 (1965)]. There is at present, however, no evidence that concentrations of antimatter exist in or near our galaxy; hence we shall disregard this possibility in our calculations.

[2] M. V. K. Apparao, Nature **215**, 727 (1967); H. Aizu, Y. Fujimoto, S. Hasegawa, M. Koshiba, I. Mito, J. Nishimura, K. Yokoi, and M. Sehein, Phys. Rev. **121**, 1206 (1961); M. Teucher, H. Winzeler, and E. Lohrmann, Nuovo Cimento **3**, 228 (1956).

[3] R. C. Hartman, P. Meyer, and R. H. Hildebrand, J. Geophys. Res. **70**, 2713 (1965); R. C. Hartman, Astrophys. J. **150**, 371 (1967).

of antiproton production.[4] By calculating the ratio of antiprotons to positrons we can largely eliminate the first difficulty. Since the same cosmic-ray distribution and ambient matter produce both particles, astrophysical uncertainties cancel. The production ratio of $\bar{p}$ to e^+ is shown to depend only on the ratio of $\bar{p}$ to π^+ (which decays to e^+) production cross sections. The former is deduced from the empirically known pion production cross section following a simple physical argument relating the two production processes. The antiproton flux at earth is then obtained by normalizing the final results to the observed positron flux. This approach has two advantages. First, at low energies (a few BeV), where the equilibrium e^+ spectrum is expected to deviate little from the production spectrum, a measurement of the $\bar{p}$ flux would serve to check the validity of the method used to calculate the $\bar{p}$ production cross section. Second, at high energies, the equilibrium ratio of $\bar{p}$ to e^+ will deviate significantly from the production ratio due to modulation in the galaxy; thus a known production ratio coupled with measurement of the equilibrium ratio would aid the study of cosmic-ray propagation.

The principal processes which produce pions and antiprotons in the interaction of cosmic-ray particles with the ambient medium include p-p, p-α, and α-p collisions.[5] Provided the incident-particle energy is much larger than nuclear binding energies, the ratio of pion to antiproton production depends weakly on the nuclei involved. Thus we can limit ourselves to p-p collisions in calculating this ratio, and generalize the final result to the total π^+ production from all processes.

The production rate of secondary particles of type x due to collisions of cosmic-ray protons of intensity $I_p(E_p)=K_pE^{-\alpha}$ with ambient hydrogen of density n atoms per cc is given by

$$Q_x(E)=4\pi n\int_{E_x^0}^{\infty}\sigma_x(E_p)f_x(E,E_p)I_p(E_p)dE_p, \quad (1)$$

where $\sigma_x(E_p)$ is the total cross section (including multiplicities) for the production of x from an incident proton with kinetic energy E_p, E_x^0 is the threshold proton energy for the production of x, E is the kinetic energy of x, and $f_x(E,E_p)$ is the energy distribution of the secondary particles. Because of the power-law nature of the cosmic-ray proton spectrum, $Q_x(E)$ is insensitive to the form of the distribution function $f_x(E,E_p)$ provided σ_x does not vary too rapidly with E_p. Thus for pion production with $E_\pi\gtrsim 1$ BeV a δ-function distribution gives satisfactory results.[6] In the production of low-energy antiprotons, however, the validity of this approximation should be checked since $\sigma_{\bar{p}}(E_p)$ rises sharply with increasing proton energy near the threshold. Hence we have calculated the antiproton production spectrum for two energy distributions:

$$f_{\bar{p}}^{(1)}(E,E_p)=\delta(E-\bar{E}_{\bar{p}}) \quad (2a)$$

and

$$f_{\bar{p}}^{(2)}(E,E_p)=(\pi E/2\bar{E}_{\bar{p}}^2)\exp[-\pi E^2/4\bar{E}_{\bar{p}}^2], \quad (2b)$$

where $\bar{E}_{\bar{p}},(E_p)$ is the mean energy of the antiprotons produced by protons of incident energy E_p. The second distribution represents closely the experimental data at accelerator energies ($E_p<30$ BeV). The corresponding equilibrium spectra are plotted in Fig. 2 as $I_{\bar{p}}^{(1)}$ and $I_{\bar{p}}^{(2)}$, respectively. As expected, there is considerable difference at lower energies ($E<2$ BeV), but above 2 BeV the two distributions give practically the same result. Since the flux drops rapidly below 1.5 BeV, the discrepancy due to the choice of $f_{\bar{p}}$ is of no experimental consequence. Thus we shall present a detailed analysis only for the δ-function energy distribution.

The mean energy of the secondaries is taken to vary as

$$\bar{E}_x(E_p)=a_xE_p^{3/4}. \quad (3)$$

The dependence on E_p is consistent with Fermi's statistical model[7] and has been experimentally verified for pions[5] above $E_p\approx 1$ BeV (about twice the threshold for pion-pair production). Experimental information is too scarce to check this relationship for antiprotons but we shall assume that it is valid in the energy range of interest ($E_p\gtrsim 20$ BeV; corresponding to $E_{\bar{p}}\gtrsim 2$ BeV). The coefficients a_x are determined from experimental data[5,8] to be $a_\pi\approx 0.175$ (BeV)$^{1/4}$ and $a_{\bar{p}}\approx 0.25$ (BeV)$^{1/4}$.

Combining Eqs. (1), (2a), and (3) gives the production rates

$$Q_x(E)=(\tfrac{1}{3}16\pi)nK_pa_x^{4(\alpha-1)/3}E^{-(4\alpha-1)/3}\sigma_x[(E/a_x)^{4/3}]. \quad (4)$$

In order to compare the ratio of antiproton to positron production, the $\pi^+\rightarrow\mu^+\rightarrow e^+$ process must be considered. For the energy range in which we are interested the positrons produced in the π decay process are given by[6]

$$Q_{e^+}(E)=(3m_\pi/m_\mu)Q_{\pi^+}(3m_\pi E/m_\mu). \quad (5)$$

The production ratio is

$$\frac{Q_{\bar{p}}(E)}{Q_{e^+}(E)}=\left(\frac{3m_\pi a_{\bar{p}}}{m_\mu a_\pi}\right)^{4(\alpha-1)/3}\frac{\sigma_{\bar{p}}[(E/a_{\bar{p}})^{4/3}]}{\sigma_{\pi^+}[(3m_\pi E/m_\mu a_\pi)^{4/3}]}$$
$$=32\frac{\sigma_{\bar{p}}[(4E)^{4/3}]}{\sigma_{\pi^+}[(22.6E)^{4/3}]}. \quad (6)$$

[4] M. I. Fradkin, Zh. Eksperim. i Teor. Fiz. **29**, 147 (1956) [English transl.: Soviet Phys.—JETP **2**, 87 (1956)]; V. L. Ginzburg, L. V. Kurnosova, L. A. Razorenov, and M. I. Fradkin, Space Sci. Rev. **2**, 778 (1963); S. Hayakawa, in *Lectures in Astrophysics and Weak Interactions* (Brandeis University Press, Waltham, Mass., 1964), Vol. 2; S. Rosen, Phys. Rev. **158**, 1227 (1967).

[5] R. Ramaty and R. E. Lingenfelter, J. Geophys. Res. **71**, 3687 (1966).

[6] R. J. Gould and G. R. Burbidge, in *Handbuch der Physik*, edited by S. Flügge (Springer-Verlag, Berlin, 1967), Vol. 46/2.

[7] E. Fermi, Progr. Theoret. Phys. (Kyoto) **5**, 570 (1950).

[8] W. F. Baker, R. L. Cool, E. W. Jenkins, T. F. Kycia, S. J. Lindenbaum, W. A. Love, D. Lüers, J. A. Niederer, S. Ozaki, A. L. Read, J. J. Russell, and L. C. L. Yuan, Phys. Rev. Letters **7**, 101 (1961); D. Dekkers, J. A. Geibel, R. Mermod, G. Weber, T. R. Willitts, K. Winter, B. Jordan, M. Vivargent, N. M. King, and E. J. N. Wilson, Phys. Rev. **137**, B962 (1965); L. G. Ratner, K. W. Edwards, C. W. Akerlof, D. G. Grabb, J. L. Day, A. D. Krisch, and M. T. Lin, Phys. Rev. Letters **18**, 1218 (1967).

The coefficient 32 is obtained by taking $\alpha=2.5$. Except for this dependence on α, all astrophysical quantities have been eliminated, and $Q_{\bar{p}}/Q_{e^+}$ depends only on the ratio of the $\bar{p}$ and π^+ production cross sections.

While σ_{π^+} is fairly well known from accelerator experiments up to $E_p\approx 30$ BeV and from cosmic-ray experiments at higher energies, measurements of the $\bar{p}$ production cross section are scarce. To complicate the problem even further only differential cross sections are measured, at angles near the forward direction. The results are too sketchy to deduce the total $\bar{p}$ production cross section without assuming a model. From the theoretical point of view the statistical model, first proposed by Fermi,[7] is perhaps the most attractive. It should give correct results at very high energies, but at energies of a few tens of BeV experimental results indicate discrepancies from the model. Several attempts have been made[9] to improve the theory with varying degrees of success. In view of the presently limited knowledge of elementary-particle interactions it is difficult to assess the value of sophisticated theoretical treatments of particle production. In the following we propose a semiempirical approach, based on rather simple physical assumptions, which allows $\sigma_{\bar{p}}(E_p)$ to be deduced from $\sigma_{\pi^-}(E_p)$.

We first note that for proton-proton collisions there is a one-to-one correspondence between processes which produce $\pi^+\pi^-$ pairs and those which produce $p\bar{p}$ pairs. For example, the reactions which require the least energy in each case are

$$p+p\rightarrow p+p+\pi^++\pi^-$$

and

$$p+p\rightarrow p+p+p+\bar{p}.$$

Since the strong interaction is responsible for production of both particle-antiparticle pairs, and the kinematics of the processes are similar except for the masses of the secondary particles, we assume that

$$\sigma_{\bar{p}}(E_p)=k\sigma_{\pi^-}(E_p'), \tag{7}$$

where E_p and E_p' are related such that the excess kinetic energy above threshold, measured in units of the rest mass of the secondary particles, is the same for each process,[10] i.e.,

$$(E_p-E_{\bar{p}}{}^0)/m_p=(E_p'-E_{\pi^-}{}^0)/m_\pi. \tag{8}$$

The constant k is determined from

$$\lim_{E\rightarrow\infty}(\sigma_{\bar{p}}/\sigma_{\pi^-})=(\lambda\!\!\!^{-}_{\bar{p}}/\lambda\!\!\!^{-}_{\pi^-})^2,$$

where $\lambda\!\!\!^{-}=\hbar/mc$; thus $k=2.22\times10^{-2}$. Inserting numerical values, we obtain

$$\sigma_{\bar{p}}(E_p)=2.22\times10^{-2}\sigma_{\pi^-}[0.149(E_p-5.63)+0.60], \tag{9}$$

where E_p is to be measured in BeV. The pion production cross sections, which have been summarized by Ramaty and Lingenfelter,[5] are plotted in Fig. 1 together with the antiproton production cross section calculated from Eq. (9), based on the same pion production data. Note that $\sigma_{\bar{p}}$ approaches the statistical model dependence $\sigma_{\bar{p}}\propto E_p^{1/4}$ for $E_p\gtrsim 300$ BeV. The available laboratory data on $\bar{p}$ production are also shown for comparison. The excellent agreement seems to support the model used. The experimental values, however, must be viewed with some reservation because they are usually given as ratios of $N_{\bar{p}}/N_{\pi^-}$ for a range of momenta at a fixed laboratory angle θ. Integration over the momenta gives $N_{\bar{p}}(\theta)/N_{\pi^-}(\theta)$. A detailed description on the conversion process is given in the Appendix. As is evident from Fig. 1, the dependence of this ratio on θ is rather weak; hence we expect $N_{\bar{p}}(\theta)/N_{\pi^-}(\theta)\approx N_{\bar{p}}/N_{\pi^-}$; and the points shown give a good estimate of $\sigma_{\bar{p}}$. We might add here that the same procedure also gives correct estimation for $\sigma_{\bar{k}}$. Note also that at 20–30 BeV there is no discernable variation of $N_{\bar{p}}/N_{\pi^-}$ in going from a hydrogen target to complex-nucleus targets. This supports the assumption that the $\bar{p}$ to e^+ ratio calculated for p-p collisions represents the ratio for the production in all processes.

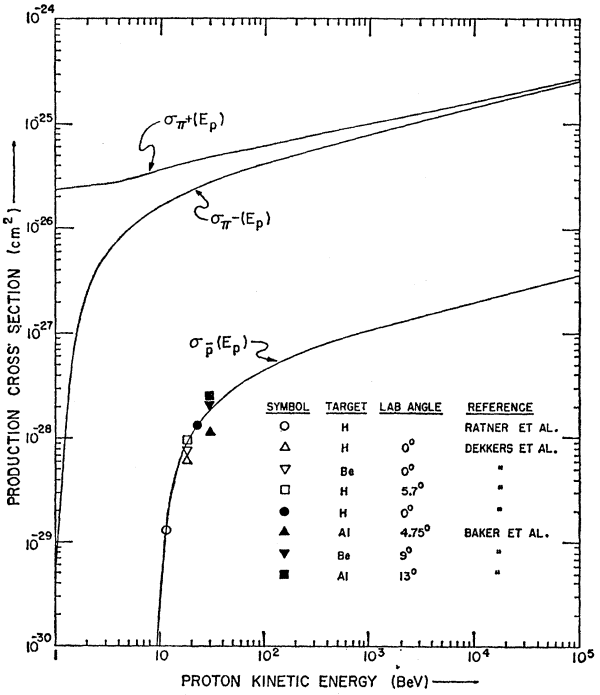

FIG. 1. Antiproton and charged-pion production cross sections (including multiplicities) for proton-proton collisions. The $\bar{p}$ curve was deduced from the π^- curve. For the point ○, the ratio was measured at fixed c.m. longitudinal momentum rather than at fixed lab angle.

[9] See, e.g., J. R. Wayland and T. Bowen, Nuovo Cimento **48A**, 663 (1967); see also the excellent review by R. Hagedorn, Nuovo Cimento Suppl. 3, 147 (1965).

[10] The negative-pion production cross section is chosen because positive pions may be produced in processes other than pair production, such as $p+p\rightarrow p+n+\pi^+$.

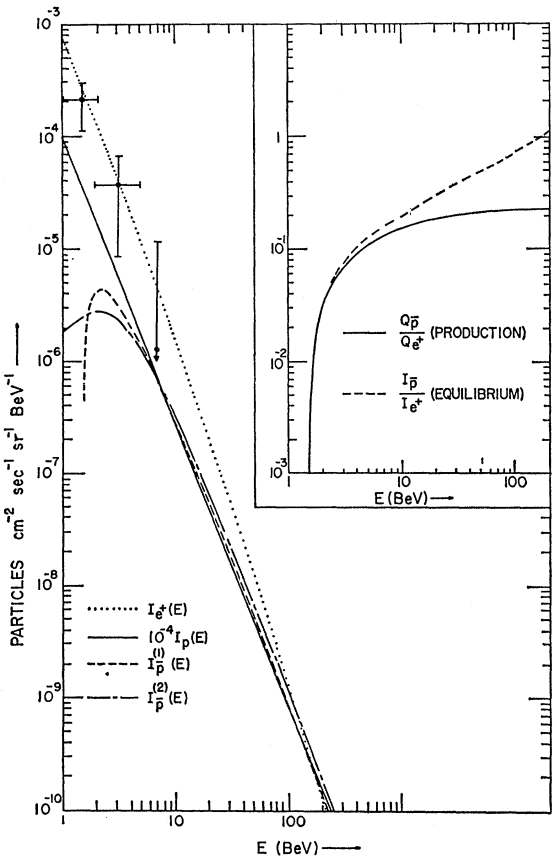

FIG. 2. The equilibrium differential energy spectra at earth for cosmic-ray protons, positrons, and antiprotons. The antiproton spectra $I_{\bar{p}}^{(1)}$ and $I_{\bar{p}}^{(2)}$ correspond, respectively, to the distribution functions $f_{\bar{p}}^{(1)}$ and $f_{\bar{p}}^{(2)}$ given by Eq. (2). The proton spectrum is multiplied by 10^{-4} for comparison with the antiproton spectrum. The points shown are measurements of the positron flux taken from Ref. 3. Inset: The ratio of antiprotons to positrons as a function of energy at production and at equilibrium.

We are now in a position to calculate $Q_{\bar{p}}(E)/Q_{e^+}(E)$ from Eq. (6). The result is shown in Fig. 2. This ratio drops rapidly below 1.5 BeV and approaches 0.25 asymptotically at large energies.

While the production ratio is independent of astrophysical parameters, the equilibrium intensity ratio observed at earth is not. In general, the equilibrium spectrum is related to the production spectrum by the diffusion equation

$$\frac{N_x}{T}-\nabla\cdot(D\nabla N_x)+\frac{\partial}{\partial E}\left[\frac{\langle\Delta E\rangle}{\Delta t}N_x - \frac{1}{2}\frac{\partial}{\partial E}\left(\frac{\langle\Delta E\rangle^2}{\Delta t}N_x\right)\right]=Q_x. \quad (10)$$

The terms on the left-hand side of Eq. (10) describe, respectively, the removal, the diffusion, and the regular and statistical acceleration of cosmic-ray particles. For positrons with energy less than about 10 BeV, escape from the galaxy dominates other effects and the production spectrum is preserved.[6] In this case

$$N(E)\approx\frac{T}{V}\int Q(E,\mathbf{r})d\mathbf{r}, \quad (11)$$

where T is the confinement time, V is the confinement volume, and the integration is over all source regions. For energies greater than 10 BeV, energy losses due to radiation become important and the spectrum steepens. The magnitude of the deviation from the production spectrum depends on the model of source distribution one chooses.[11] Diffusion of antiprotons is similar to that of protons except for the additional possibility of annihilation. But this is unimportant for passing 3 g/cm² of mass. The only process which might alter the antiproton energy spectrum is acceleration in interstellar space.[12] However, the shape of the antiproton production spectrum is, except at low energies, very similar to the local proton spectrum, so that even if acceleration is efficient the equilibrium spectra of antiprotons and protons should still be similar.

The absolute intensity of the antiproton flux can be obtained by comparison with the observed positron intensity at a few BeV. In this energy range they are both related to the respective production spectra through Eq. (11). Assuming that both particles are produced in the same sources and confined in the same region, we have, for $E<10$ BeV, $I_{\bar{p}}(E)/I_{e^+}(E)\simeq Q_{\bar{p}}(E)/Q_{e^+}(E)$, independent of the exact manner of propagation of cosmic rays. The theoretical antiproton energy spectra $I_{\bar{p}}(E)$ are plotted in Fig. 2 together with the proton spectrum (displaced downward by 10^{-4}) and the positron spectrum (based on the experimental data[3] and a galactic disk source distribution with halo confinement[11]). Above 10 BeV the antiproton flux is about 10^{-4} of the proton flux. At lower energies the antiproton spectrum levels off, and the antiproton-proton ratio becomes less than 10^{-5} below 1.5 BeV.

In the past several attempts have been made to detect antiprotons in cosmic rays. They have resulted in an upper limit of a few times 10^{-4} for the antiproton to proton ratio.[2] These experiments are, however, aimed at low-energy ($E<1$ BeV) antiprotons. As indicated in Fig. 2, the most favorable energy range for observation of antiprotons is around a few BeV.

Since in this energy range the intensity ratio of antiproton to positron depends only upon the production cross sections, a direct detection of cosmic-ray antiprotons would test the validity of the collision model [Eqs. (7) and (8)] used in the calculation. This might be helpful in the theoretical study of the production cross section of other hypothetical massive particles. Measurement of antiprotons at higher energy ($E_{\bar{p}}\geq 10$ BeV), which is perhaps beyond present experimental grasp due

[11] C. S. Shen, Phys. Rev. Letters **19**, 399 (1967).
[12] J. R. Wayland and T. Bowen (to be published).

to the low intensity, would provide a unique probe in the study of the origin and propagation of cosmic-ray particles.

APPENDIX

In this Appendix we give the conversion of experimental data to the points plotted in Fig. 1.

Experimental measurements give $\partial^2\sigma(E_p)/\partial\Omega\partial P$ for a range of momenta at a fixed laboratory angle Ω. To convert these directly measured values into the experimental points plotted in Fig. 1, one must first integrate $\partial^2\sigma(E_p)/\partial\Omega\partial P$ over the momenta to give $\partial\sigma(E_p)/\partial\Omega$ and then calculate $\sigma_{\bar{p}}$ from σ_{π^-} by comparing $\sigma_{\bar{p}}(E_p)/\sigma_{\pi^-}(E_p)$ with

$$\frac{[\partial\sigma_{\bar{p}}(E_p)/\partial\Omega]}{[\partial\sigma_{\pi^-}(E_p)/\partial\Omega]}.$$

To illustrate the method used we shall present the calculation in detail for two of the experimental points in Fig. 1.

(1) The point △ in Fig. 1 is from Dekkers's experiment[8] for incident-proton momentum 18.8 BeV/c (corresponding to $E_p=17.9$ BeV), laboratory angle $\theta=0$ and proton target. The data are given in Table I.

TABLE I. Differential cross sections for $\bar{p}$ and π^- production in p-p collision at incident energy of 17.9 BeV and laboratory angle of 0°. The values are from Dekkers *et al.*,[a] except for those denoted by an asterisk, which were derived from measurements at higher laboratory momentum.

P (BeV/c)	$\partial^2\sigma_{\bar{p}}/\partial P\partial\Omega$ (mb(BeV/c)$^{-1}$sr^{-1})	$\partial^2\sigma_{\pi^-}/\partial P\partial\Omega$ (mb(BeV/c)$^{-1}$sr^{-1})
0.05		0.27±0.03*
0.17		3.36±0.40*
1.0		26.2 ±3.2
1.15	0.012±0.002*	
2.0		30.0 ±3.0
2.24	0.082±0.025*	
3.0		34.0 ±3.4
4.0	0.154±0.046	28.0 ±4.0
6.0	0.077±0.022	21.6 ±1.7
8.0		13.3 ±0.9
10.0		7.8 ±0.5
12.0		2.45±0.2

[a] See Ref. 8.

The superscript b following an entry indicates that the cross section has been derived from a measurement at higher laboratory momentum. This is possible because in this special case we are dealing with p-p collisions at 0°. Since in the center-of-momentum frame

$$\left.\frac{\partial^2\sigma_c}{\partial P_c\partial\Omega_c}\right|_{\theta_c=0^\circ}=\left.\frac{\partial^2\sigma_c}{\partial P_c\partial\Omega_c}\right|_{\theta_c=180^\circ},$$

we can therefore convert data of higher laboratory momenta (corresponding to $\theta_c=0°$) into their mirror points at lower laboratory momenta (corresponding to $\theta_c=180°$). The data of Table I can be integrated numerically to give $d\sigma_{\pi^-}/d\Omega$ and $d\sigma_{\bar{p}}/d\Omega$. The ratio is

$$\frac{d\sigma_{\bar{p}}}{d\Omega}\Big/\frac{d\sigma_{\pi^-}}{d\Omega}=2.7\times10^{-3} \quad \text{at} \quad \theta=0^\circ.$$

Since the total production cross section for π^- is σ_{π^-} (17.9 BeV)$=2\times10^{-26}$cm^2, we have $\sigma_{\bar{p}}$(17.9 BeV) $\approx2\times10^{-26}\times2.7\times10^{-3}\simeq5.4\times10^{-29}$ cm^2. Notice that the other two points (□ and ▽) obtained at the same incident energy (but at different angle or with different target) are consistent with this value.

(2) The point ○ in Fig. 1 is based on Ratner's[8] data. Since their measurement is given at fixed c.m. longitudinal momentum instead of at fixed lab angle, integration over the transverse momentum gives directly $\sigma_{\bar{p}}/\sigma_{\pi^-}$ at the particular longitidinal momentum. From their Fig. 2 we have

$$\sigma_{\pi^-}(p_\perp)dp_\perp=2.5\times10^3\exp[-(3.5p_\perp{}^2)]\times\mu\text{b(BeV}/c)^{-1}\text{ sr}^{-1},$$

$$\sigma_{\bar{p}}(p_\perp)dp_\perp=2.5\exp[-(7p_\perp{}^2)]\mu\text{b(BeV}/c)^{-1}\text{sr}^{-1},$$

$$\sigma_{\bar{p}}/\sigma_{\pi^-}=\int\sigma_{\bar{p}}dp_\perp\Big/\int\sigma_\pi dp_\perp=7\times10^{-4}.$$

This gives $\sigma_{\bar{p}}$ (11.6 BeV)$=1.2\times10^{-29}$ cm^2.